Code Random Access and Blind Source Separation for Massive Machine Type Communications

Michele Godeas[1], Alberto Carini[1], Fulvio Babich[1], Lorenzo Valentini[2], and Enrico Paolini[2]
[1] Department of Engineering and Architecture - University of Trieste, Trieste, Italy
[2] Department of Electrical, Electronic and Information Engineering "G. Marconi," CNIT, University of Bologna, Italy

***Abstract*—This paper investigates the use of blind source separation (BSS) in conjunction with coded random access (CRA) for diversity ALOHA in massive machine-type communications. A scheme for effectively integrating BSS into a CRA ALOHA framework to resolve user conflicts is presented. The achievable performance is analyzed experimentally, and the factors influencing the number of detectable users are highlighted.**

***Index Terms*—Blind source separation, Coded random access, ALOHA, Massive machine-type communications**

I. Introduction

We explore a grant-free massive multiple access (MMA) framework, where a vast number of machine-type devices intermittently become active to send short data packets to a base station (BS) equipped with M antennas, with no prior resource allocation. This communication model has emerged as a key focus in the development of next-generation massive machine-type communications (mMTC). To efficiently manage this high-density access, coded random access (CRA) techniques have been extensively investigated [1]–[8]. These methods exploit resource diversity, including variations in code and time slot allocation, while incorporating successive interference cancellation (SIC) to enable the concurrent transmission of numerous devices.

Similar to framed ALOHA, transmissions are structured into frames, each comprising a predefined number of slots. The BS broadcasts a beacon at the beginning of each frame to signal its start. The beacon is useful for both synchronization and power control purposes. Within each frame, active users compete for access to the transmission channel, randomly selecting one or more slots to send multiple copies of the same payload message, each accompanied by a pilot sequence. While non-orthogonal pilot sequences are possible, orthogonal sequences are generally preferred for their simplicity in detection and SIC. The BS utilizes knowledge of the pilot sequences to detect transmitted messages and applies SIC at both slot and frame levels [4]–[6].

In CRA with power control, when two or more users choose the same pilot sequence, detection likely fails, necessitating retransmission for another detection attempt. This paper addresses this issue by integrating CRA with a blind source separation (BSS) algorithm. First, CRA detection is performed. Then, BSS is applied to resolve conflicts in pilot assignment. The synergy between these approaches enhances message detection, reduces the number of retransmissions, and ultimately conserves energy at the user terminals.

This study assumes quadrature phase-shift keying (QPSK) modulation with Gray mapping for transmission. For this modulation scheme, the constant modulus algorithm (CMA) [9], [10] has been identified as the most effective BSS approach, as it exploits the constant modulus property of the constellation. However, its efficient implementation requires several refinements: reducing the problem size to accelerate convergence, correcting phase errors, applying a deflation method to avoid redundant solutions, and adopting strategies to mitigate the adverse effects of noise accumulation caused by deflation [11]. Additionally, all these considerations must be effectively integrated with the CRA framework. The main contribution of this paper is the derivation of an effective solution for using BSS in conjunction with CRA, achieved through the integration and adaptation of the aforementioned algorithms, along with a thorough experimental evaluation of its performance.

The remainder of the paper is structured as follows. Section II describes the considered transmission scheme, and Section III provides a detailed description of the proposed base station processing. Section IV presents simulation results, demonstrating the feasibility of the approach and its improvements over the conventional CRA method. Finally, conclusions are drawn in Section V.

II. Transmission scheme

We consider a transmission scheme structured into frames, where each frame is composed of N_{s} slots. Within each frame, K_{a} active users attempt to access the transmission channel without prior knowledge of K_{a} at the BS. Each user independently and randomly selects R slots to send multiple copies of its payload and assigns a pilot sequence to each transmission slot at random[1]. The pilot sequences are drawn from a predefined set of N_{P} orthogonal sequences, aiding in both channel estimation and packet decoding.

The payload comprises the information bits, a cyclic redundancy check (CRC) for error detection, and redun-

This work was partially supported by the European Union - Next Generation EU under the Italian National Recovery and Resilience Plan (NRRP), Mission 4, Component 2, Investment 1.3, CUP J33C22002880001 and CUP D93C22000910001, partnership on "Telecommunications of the Future" (PE00000001 - program "RESTART").

[1]As explained below, if the BS acknowledges receipt of a message, the user will not transmit the remaining replicas of the payload.

dancy due to channel encoding for reliability enhancement. For instance, the experimental results incorporate a Bose–Chaudhuri–Hocquenghem (BCH) code for encoding. The selection of the R slots can be deterministically derived from a pseudo-random function based on the transmitted message, enabling the BS to infer the slot positions upon successful message decoding. Alternatively, the payload may explicitly convey the chosen slot positions.

Each transmitted message undergoes modulation before being sent to the BS. To facilitate BSS, QPSK modulation with Gray mapping is employed in this paper. The communication channel is modeled as a block fading channel, where the coherence time matches the slot duration. Consequently, the channel coefficients remain unchanged throughout the transmission of a packet within a given slot. Perfect power control is assumed; therefore, packets arrive at the receiver with the same power.

III. Base Station Processing

The following sub-sections provide a mathematical formulation of the proposed approach, showing how the problem size can be reduced by estimating the number of active users per slot. The detection steps are discussed in the order in which they are applied: first, CRA detection and intra-slot successive interference cancellation (SIC); then, the selected BSS technique with the double gradient descent (DGD) method used to enhance detection; finally, intra-frame SIC and the end-of-frame detection process.

A. Mathematical formulation of the problem

On the receiver side, the signal received by the M antennas of the BS in a slot can be expressed as $[\mathbf{P}, \mathbf{Y}] \in \mathbb{C}^{M\times(N_\mathrm{P}+N_\mathrm{D})}$, where [12]:

$$\mathbf{P} = \sum_{k=1}^{N_\mathcal{A}} \mathbf{h}_k \mathbf{s}_k + \mathbf{Z}_p, \tag{1}$$

$$\mathbf{Y} = \sum_{k=1}^{N_\mathcal{A}} \mathbf{h}_k \mathbf{x}_k + \mathbf{Z}_y, \tag{2}$$

N_P is the pilot length, N_D is the payload length, and $N_\mathcal{A}$ represents the number of users transmitting a packet within the given slot. The channel vector for user k is denoted by $\mathbf{h}_k \in \mathbb{C}^{M\times 1}$, where its components are independent and identically distributed (i.i.d.) random variables drawn from a circularly symmetric complex Gaussian distribution with zero mean and variance σ_h^2, i.e., $\mathcal{CN}(0, \sigma_h^2)$. Due to power control, we assume without loss of generality that $\sigma_h^2 = 1$ for all users. The matrices $\mathbf{Z}_p \in \mathbb{C}^{M\times N_\mathrm{P}}$ and $\mathbf{Z}_y \in \mathbb{C}^{M\times N_\mathrm{D}}$ model additive noise, where their elements are i.i.d. random variables following a complex Gaussian distribution $\mathcal{CN}(0, \sigma_\nu^2)$, with σ_ν^2 representing the noise variance. Equations (1) and (2) can also be expressed in matrix form as:

$$\mathbf{P} = \mathbf{H}\mathbf{S} + \mathbf{Z}_p, \tag{3}$$

$$\mathbf{Y} = \mathbf{H}\mathbf{X} + \mathbf{Z}_y, \tag{4}$$

where $\mathbf{H} = [\mathbf{h}_1, \ldots, \mathbf{h}_{N_\mathcal{A}}]$ is a matrix with channel vectors $\mathbf{h}_k$ as columns, $\mathbf{H} \in \mathbb{C}^{M\times N_\mathcal{A}}$, $\mathbf{S} = [\mathbf{s}_1^T, \ldots, \mathbf{s}_{N_\mathcal{A}}^T]^T$ is a matrix with prefix sequences $\mathbf{s}_k$ as rows, $\mathbf{S} \in \mathbb{C}^{N_\mathcal{A}\times N_\mathrm{P}}$, and $\mathbf{X} = [\mathbf{x}_1^T, \ldots, \mathbf{x}_{N_\mathcal{A}}^T]^T$ is a matrix with payload sequences $\mathbf{x}_k$ as rows, $\mathbf{X} \in \mathbb{C}^{N_\mathcal{A}\times N_\mathrm{D}}$.

The CRA and BSS algorithms aim to iteratively determine a separating vector $\mathbf{d}_k$ such that the projection $\mathbf{d}_k^H\mathbf{Y}$ closely approximates one of the sequences $\mathbf{x}_k$, where $k \in \{1, \ldots, N_\mathcal{A}\}$. In the BSS procedure, the inherent symmetry of the QPSK constellation introduces an ambiguity factor of $e^{jm\pi/2}$, for $m \in \{0, \ldots, 3\}$, in the estimation of $\mathbf{x}_k$. This phase uncertainty can be resolved either by assuming prior knowledge of the first transmitted symbol or by leveraging the CRC code embedded in the payload.

B. Problem size reduction

The BSS problem is addressed using a gradient descent method. The convergence rate of gradient-based techniques is inversely related to the number of unknown coefficients. To accelerate convergence, we reduce the dimensionality of the problem. This is achieved by merging the matrices $\mathbf{P}$ and $\mathbf{Y}$ into a unified matrix, enabling the reformulation of equations (4) and (3) as:

$$[\mathbf{P}, \mathbf{Y}] = \mathbf{H} \cdot [\mathbf{S}, \mathbf{X}] + [\mathbf{Z}_p, \mathbf{Z}_y]. \tag{5}$$

The Singular Value Decomposition (SVD) of $[\mathbf{P}, \mathbf{Y}]$ is then computed as:

$$[\mathbf{P}, \mathbf{Y}] = \mathbf{U}\mathbf{\Sigma}\mathbf{V}^H, \tag{6}$$

where $\mathbf{U} \in \mathbb{C}^{M\times M}$ and $\mathbf{V} \in \mathbb{C}^{N\times N}$, with $N = N_\mathrm{P} + N_\mathrm{D}$, and $\mathbf{\Sigma}$ is an $M \times N$ diagonal matrix of singular values.

The matrix $\mathbf{\Sigma}$ is formed by $N_\mathcal{A}$ large singular values and $M - N_\mathcal{A}$ smaller ones generated by noise. By neglecting the smaller singular values, we can consider the matrix:

$$[\widetilde{\mathbf{P}}_1, \widetilde{\mathbf{Y}}_1] = \mathbf{\Sigma}_{[1,N_\mathcal{A}]}\mathbf{V}^H_{[1,N_\mathcal{A}]}, \tag{7}$$

where $\mathbf{\Sigma}_{[1,N_\mathcal{A}]}$ is the diagonal matrix formed by the $N_\mathcal{A}$ largest singular values, $\mathbf{V}_{[1,N_\mathcal{A}]}$ is the matrix containing the corresponding columns of $\mathbf{V}$, $\widetilde{\mathbf{P}}_1$ is a $N_\mathcal{A}\times N_\mathrm{P}$ matrix and $\widetilde{\mathbf{Y}}_1$ is a $N_\mathcal{A}\times N_\mathrm{D}$ matrix. The BSS problem is equivalent to finding a separating vector $\widetilde{\mathbf{d}}_k$ such that $\widetilde{\mathbf{d}}_k^H\widetilde{\mathbf{Y}}_1$ closely approximates one of the payload sequences $\mathbf{x}_k$. Moreover, it can be shown that the CRA approach can equivalently use $\widetilde{\mathbf{P}}_1$ and $\widetilde{\mathbf{Y}}_1$ in place of $\mathbf{P}$ and $\mathbf{Y}$, respectively.

Eq. (7) requires the knowledge of $N_\mathcal{A}$. The number of active users is here efficiently estimated from the normalized forward difference (NFD) of the singular values [11]:

$$N_\mathcal{A} = \arg\max_i \left\{ \frac{\sigma_i - 2\sigma_{i+1} + \sigma_{i+2}}{1 + \sigma_i} \right\}, \tag{8}$$

where σ_i represents the i-th singular value of $\mathbf{Y}$, arranged in descending order. The denominator term prevents issues with near-zero divisions at high SNR.

C. The CRA detection

The approach of [6] is applied. In each slot, the BS attempts to estimate the payload by computing, for each orthogonal pilot sequence $\mathbf{s}_l$, the following vectors:

$$\boldsymbol{\phi}_l = \frac{\widetilde{\mathbf{P}}_1\mathbf{s}_l^H}{\|\mathbf{s}_l\|^2} = \sum_{k\in\mathcal{A}_l} \widetilde{\mathbf{h}}_k + \mathbf{z}_l, \tag{9}$$

$$\mathbf{f}_l = \boldsymbol{\phi}_l \widetilde{\mathbf{Y}}_j = \sum_{k\in\mathcal{A}_l} \|\widetilde{\mathbf{h}}_k\|^2 \mathbf{x}_k + \sum_{k\in\mathcal{A}_l} \sum_{\substack{m=1\\ m\neq k}}^{N_\mathcal{A}} \widetilde{\mathbf{h}}_k^H \widetilde{\mathbf{h}}_m \mathbf{x}_m + \hat{\mathbf{z}}_l, \tag{10}$$

$$g_l = \|\boldsymbol{\phi}_l\|^2 = \sum_{k\in\mathcal{A}_l} \|\widetilde{\mathbf{h}}_k\|^2 + \sum_{k\in\mathcal{A}_l} \sum_{\substack{m=1\\ m\neq k}}^{N_\mathcal{A}} \widetilde{\mathbf{h}}_m^H \widetilde{\mathbf{h}}_k + \hat{n}_l, \tag{11}$$

and

$$\widehat{\mathbf{x}}_l = \frac{\mathbf{f}_l}{g_l} = \frac{\boldsymbol{\phi}_l \widetilde{\mathbf{Y}}_j}{\|\boldsymbol{\phi}_l\|^2}, \tag{12}$$

where $\boldsymbol{\phi}_l \in \mathbb{C}^{M\times 1}$, $\mathbf{f}_l$ and $\widehat{\mathbf{x}}_l \in \mathbb{C}^{1\times N_\mathrm{D}}$, and $g_l \in \mathbb{C}$. In (9)–(11), $\mathcal{A}_l \subseteq \mathcal{A}$ represents the subset of active users adopting pilot l in the current slot, $\widetilde{\mathbf{h}}_k = \mathbf{U}^H_{[1,N_\mathcal{A}]}\mathbf{h}_k$, and $\mathbf{z}_l \in \mathbb{C}^{M\times 1}$, $\hat{\mathbf{z}}_l \in \mathbb{C}^{M\times 1}$, and $\hat{n}_l \in \mathbb{C}$ are additive noise vectors. In (10) and (12), j is initially set to 1 but is incremented after each intra-slot SIC. By projecting $\widehat{\mathbf{x}}_l$ onto the constellation symbols, applying error correction, and verifying the CRC code, a payload sequence $\mathbf{x}_j$ can be detected.

D. Post-CRA intra-slot signal interference cancellation

Whenever a payload sequence $\mathbf{x}_j$ is identified, intra-slot SIC is performed. The process begins with $j = 1$, and the deflated matrix is updated as

$$\widetilde{\mathbf{Y}}_{j+1} = \widetilde{\mathbf{Y}}_j - \widetilde{\mathbf{h}}_j \mathbf{x}_j, \tag{13}$$

where the channel vector $\widetilde{\mathbf{h}}_j \in \mathbb{C}^{N_\mathcal{A}\times 1}$ is given by the previously computed vector in (9). By applying intra-slot SIC, the likelihood of detecting the same sequence with the BSS algorithm is reduced and the detection accuracy is improved. Moreover, SIC is applied only to the matrix $\widetilde{\mathbf{Y}}_1$, while in this phase it can be skipped for the matrix $\widetilde{\mathbf{P}}_1$ due to the orthogonality of the pilot sequences.

E. The BSS algorithm

Whenever two or more users select the same pilot sequence, CRA detection fails for these users. However, the BSS algorithm can be used to retrieve their payload messages.

Given $\widetilde{\mathbf{Y}}_j$, the goal is to determine the $N_\mathcal{A} \times 1$ separating vector $\widetilde{\mathbf{d}}$ such that the components of $\widetilde{\mathbf{d}}^H \widetilde{\mathbf{Y}}_j$ closely resemble the QPSK constellation. To achieve this, the constant modulus algorithm (CMA) [9], [10] is employed. The CMA aims at minimizing the cost function:

$$J(\widetilde{\mathbf{d}}) = \frac{1}{N} \sum_{n=1}^{N} \left(\left| \widetilde{\mathbf{d}}^H \widetilde{\mathbf{y}}(n) \right|^2 - 1 \right)^2, \tag{14}$$

where $\widetilde{\mathbf{y}}(n)$ represents the n-th column of $\widetilde{\mathbf{Y}}_j$.

The optimization is carried out using a gradient descent approach, initialized with a random $N_\mathcal{A} \times 1$ vector $\widetilde{\mathbf{d}}_{(0)}$ that is updated iteratively according to:

$$\widetilde{\mathbf{d}}_{(i+1)} = \widetilde{\mathbf{d}}_{(i)} - \mu \nabla J, \tag{15}$$

where [13]

$$\nabla J = \frac{2}{N} \sum_{n=1}^{N} \left(\left| \widetilde{\mathbf{d}}_{(i)}^H \widetilde{\mathbf{y}}(n) \right|^2 - 1 \right) \left(\widetilde{\mathbf{d}}_{(i)}^T \widetilde{\mathbf{y}}^*(n) \right) \widetilde{\mathbf{y}}(n). \tag{16}$$

To accelerate convergence, the optimal step-size μ can be dynamically determined at each iteration using the method outlined in [14]. The gradient descent algorithm runs for a maximum of I iterations, halting once all recovered symbols $\hat{x}_n = \widetilde{\mathbf{d}}^H \widetilde{\mathbf{y}}(n)$ for $n = 1, \ldots, N_\mathrm{D}$ lie within the annular region defined by $r_1 \leq |\hat{x}_n| \leq r_2$, where $r_1 = 0.6$ and $r_2 = 1.4$ in the experimental setup. To refine the recovered symbols, their phase is adjusted to align clusters with the QPSK constellation points, thereby reducing errors. This is achieved by minimizing the phase error across all symbols, solving for $\hat{\theta}$ that satisfies

$$\hat{\theta} = \min_{\theta} \sum_{n=1}^{N} \left| (e^{j\theta}\hat{x}_n)^4 + 1 \right|^2. \tag{17}$$

It can be shown that the optimal phase correction is given by

$$\hat{\theta} = -\frac{\operatorname{atan2}(B, A)}{4} + \frac{\pi}{4}, \tag{18}$$

where $A = \sum_{n=1}^{N} |\hat{x}_n|^4 \cos(4\theta_n)$, $B = \sum_{n=1}^{N} |\hat{x}_n|^4 \sin(4\theta_n)$, and $\theta_n = \arg(\hat{x}_n)$.

The phase-corrected symbols $e^{j\hat{\theta}}\hat{x}_n$ are subsequently mapped to the closest constellation points, resolving any phase ambiguity. Detection is then performed with the aid of an error-correcting code. If sequence detection is unsuccessful, the gradient descent algorithm can be re-executed up to N_T times, each iteration starting from a different randomly initialized vector $\widetilde{\mathbf{d}}_{(0)}$.

Whenever the payload sequence $\mathbf{x}_j$ is successfully identified, we apply (13) to remove an estimate of its contribution from the matrix $\widetilde{\mathbf{Y}}_j$, where the channel vector $\widetilde{\mathbf{h}}_j$ is obtained using the payload-assisted estimation method [6],

$$\widetilde{\mathbf{h}}_j = \frac{\widetilde{\mathbf{Y}}_j \mathbf{x}_j^H}{\|\mathbf{x}_j\|^2}. \tag{19}$$

To resolve user collisions it is beneficial to apply SIC also to the matrix $\widetilde{\mathbf{P}}_1$ as:

$$\widetilde{\mathbf{P}}_{j+1} = \widetilde{\mathbf{P}}_j - \widetilde{\mathbf{h}}_j \mathbf{s}_j. \tag{20}$$

where $\mathbf{s}_j$ is derived from the payload itself. Applying SIC to $\widetilde{\mathbf{P}}_1$ can facilitate the CRA detection of additional messages during the final detection phase at the end of the frame.

F. Double gradient descent approach

One of the challenges in SIC is the reduction in separation effectiveness as more signals are removed [15]. To address this limitation, we employ the DGD technique, as outlined in [11].

Suppose that j payload sequences have already been extracted, and we seek to recover the $(j+1)$-th sequence, $\mathbf{x}_{j+1}$. The method initiates with the application of CMA on the deflated matrix $\widetilde{\mathbf{Y}}_{j+1}$. The resultant parameter vector, $\hat{\mathbf{d}}_{j+1}$, serves as an initial estimate for performing another CMA descent on the original mixture, $\widetilde{\mathbf{Y}}_1$. The objective is to provide an initialization that remains unaffected by previously identified components ($\mathbf{x}_1$, ... $\mathbf{x}_j$), while being sufficiently close to the correct solution to ensure rapid convergence.

From the application of CMA on $\widetilde{\mathbf{Y}}_{j+1}$, we obtain the parameter vector $\hat{\mathbf{d}}_{j+1} \in \mathbb{C}^{N_\mathcal{A}}$, satisfying:

$$\hat{\mathbf{d}}_{j+1}^H \widetilde{\mathbf{Y}}_{j+1} = \hat{\mathbf{x}}_{j+1}. \tag{21}$$

We now seek a vector $\widetilde{\mathbf{d}}_{j+1,0}$ such that:

$$\widetilde{\mathbf{d}}_{j+1,0}^H \widetilde{\mathbf{Y}}_1 = \hat{\mathbf{d}}_{j+1}^H \widetilde{\mathbf{Y}}_{j+1} = \hat{\mathbf{x}}_{j+1}. \tag{22}$$

The vector $\widetilde{\mathbf{d}}_{j+1,0}$ will be used as the initialization point for CMA applied to $\widetilde{\mathbf{Y}}_1$. As shown later, the separating vector $\widetilde{\mathbf{d}}_j$ can be assumed to satisfy:

$$\widetilde{\mathbf{d}}_j^H \widetilde{\mathbf{Y}}_1 = \mathbf{x}_j. \tag{23}$$

Substituting (23) into (13), we obtain:

$$\widetilde{\mathbf{Y}}_{j+1} = \widetilde{\mathbf{Y}}_j - \widetilde{\mathbf{h}}_j \widetilde{\mathbf{d}}_j^H \widetilde{\mathbf{Y}}_1. \tag{24}$$

Applying this iteratively, we have:

$$\widetilde{\mathbf{Y}}_{j+1} = \mathbf{T}_{j+1} \widetilde{\mathbf{Y}}_1 \tag{25}$$

where $\mathbf{T}_{j+1} = \mathbf{T}_j - \widetilde{\mathbf{h}}_j \widetilde{\mathbf{d}}_j^H$, with an initial condition of $\mathbf{T}_1 = \mathbf{I}$, the $N_{\mathcal{A}} \times N_{\mathcal{A}}$ identity matrix.
Substituting (25) into (22), we derive $\widetilde{\mathbf{d}}_{j+1,0}^H = \hat{\mathbf{d}}_{j+1}^H \mathbf{T}_{j+1}$.

Using $\widetilde{\mathbf{d}}_{j+1,0}$ as the initial estimate for another CMA descent on $\widetilde{\mathbf{Y}}_1$ often facilitates the efficient extraction of a new sequence, $\mathbf{x}_{j+1}$. This iterative technique is referred to as the *double gradient descent*. We note that, in order to guarantee a correct behavior of the DGD method, it is crucial to update the transformation matrix $\mathbf{T}_j$ also when applying the above mentioned post-CRA SIC. An accurate estimate of the separating vector can be obtained by directly solving (23). By leveraging (7), $\widetilde{\mathbf{d}}_j$ can be efficiently computed as:

$$\widetilde{\mathbf{d}}_j^H = [\mathbf{p}_j \mathbf{x}_j]\, \widetilde{\mathbf{V}}_{[1,N_A]} \widetilde{\mathbf{\Sigma}}^{-1}_{[1,N_A]}, \tag{26}$$

where $\mathbf{p}_j$ denotes the pilot associated with $\mathbf{x}_j$.

G. Message acknowledgment

As outlined in [4], it is assumed that in each slot, following detection, the BS confirms successful decoding to users whose payloads have been correctly received. This confirmation enables users to refrain from redundant message retransmissions, leading to reduced power consumption. Additionally, [4] demonstrated that halting unnecessary retransmissions mitigates interference and enhances detection efficiency. Acknowledgments are conveyed by broadcasting the pilot codes corresponding to all successfully decoded messages, provided there are no conflicts. In the presence of conflicts, the pilot code is transmitted only if all messages associated with that pilot code have been successfully detected, where the number of colliding users can be easily estimated from (9) as $\frac{||\boldsymbol{\phi}_l||^2}{M}$.

H. Intra-frame signal interference cancellation

At the conclusion of the frame, intra-frame SIC is applied. Any detected message that has been transmitted multiple times is removed from the matrices $\widetilde{\mathbf{P}}_j$ and $\widetilde{\mathbf{Y}}_j$ in the slots where it was not initially identified. Subsequently, signal detection is reattempted using both the CRA and BSS methods. This iterative procedure may facilitate the discovery of additional payload messages, triggering a sequence of successive intra-frame SICs and detections. The process continues until either all messages have been successfully detected or no further payload messages can be identified. In the DGD algorithm, SIC necessitates an estimate of the channel $\widetilde{\mathbf{h}}_j$ and a separating vector $\widetilde{\mathbf{d}}_j$ for each message $\mathbf{x}_j$. These parameters can be determined using (19) and (26).

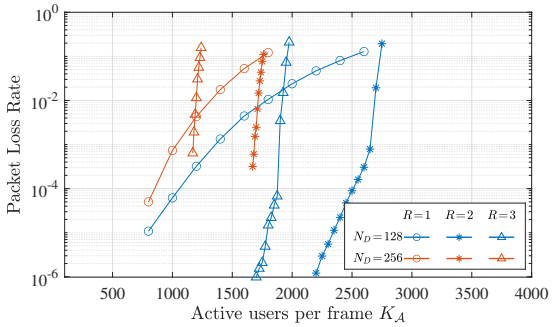

(a) BSS ALOHA

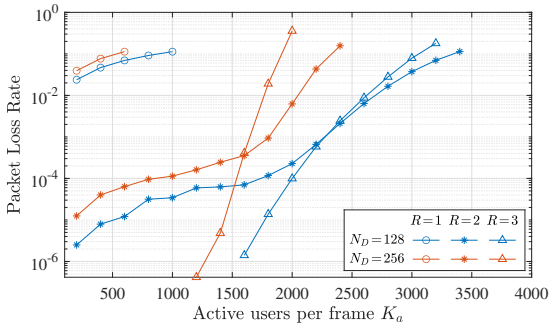

(b) CRA ALOHA

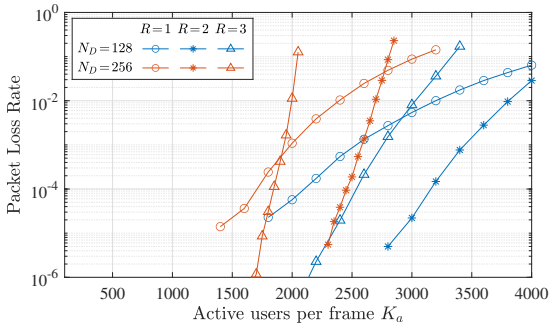

(c) CRA+BSS ALOHA

Fig. 1: Packet Loss Rate under different conditions for (a) BSS ALOHA, (b) CRA ALOHA, and (c) the proposed approach combining CRA and BSS.

IV. Simulation Results

In Fig. 1, the packet loss rate (PLR) per frame of the proposed approach is compared with the PLR of the original CRA system from [6] (without considering "spatial coupling") and with the PLR of the ALOHA system of [11], which relies solely on the BSS algorithm described in Subsections III.E and III.F and does not consider any pilot sequence. In the figure, K_a is the number of active users in the frame and each data point represents the average of 3000 runs.

The configuration settings used in the simulations are reported in Table I. Specifically, in the simulation results, the BS is assumed to be composed of $M = 256$ antennas with a signal-to-noise ratio (SNR) of 10 dB. Six different transmission conditions are considered, varying the payload length $N_D \in \{128, 256\}$ and the number of repetitions $R \in \{1, 2, 3\}$. For $R = 1$, there is no intra-frame SIC.

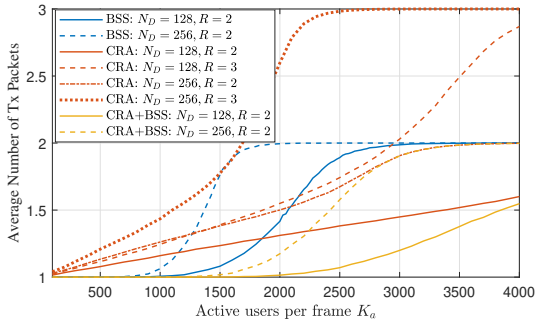

Fig. 2: Average number of transmitted packets per active user.

The frame length and the number of slots are calculated by considering the same latency constraints and symbol rate as in [12], leading to the following payload length and number of slots pairs, (N_D, N_s), for the proposed approach and the CRA ALOHA of [6]: $(128, 130)$ and $(256, 78)$. For the BSS ALOHA of [11], due to the absence of pilot sequences, a larger number of slots is available for the same frame length, resulting in (N_D, N_s) pairs of $(128, 195)$ and $(256, 97)$.

In the proposed approach and in the BSS ALOHA, the gradient descent algorithm can be re-executed up to $N_T = 4$ times with at most $I = 100$ iterations. Increasing the payload length N_D enhances the BSS algorithm's ability to detect messages but simultaneously increases the number of messages transmitted within the same slot due to the reduced number of slots. Fig 1a and 1c demonstrate that the latter effect dominates, making shorter messages more advantageous. A similar behavior is observed in the CRA ALOHA, with the best performance obtained for $N_D = 128$. Regarding the number of repetitions, the best performance is achieved with $R = 2$ for both the BSS ALOHA and the proposed approach, while $R = 3$ can be advantageous for the CRA ALOHA. Comparing the different methods, Fig. 1 shows that for $N_D = 128$, BSS ALOHA is already competitive with the CRA ALOHA. With a PLR of 10^{-4}, it can support 2500 active users per frame, compared to 2000 users per frame for CRA ALOHA. However, the proposed approach, which combines the best characteristics of CRA and BSS, provides superior performance compared to both methods, allowing more than 3000 active users per frame with a PLR of 10^{-4}.

An important aspect of the BSS approach is that it reduces the number of transmitted packets per active user and, therefore, the energy consumption of the user terminals. This can be observed in Fig. 2, which shows the average number of transmitted packets per active user for the most significant configurations of Fig. 1. The proposed approach, which combines CRA and BSS, consistently results in a lower average number of transmitted packets compared to CRA ALOHA, for the same payload length N_D and maximum number of repetitions R. Additionally, BSS ALOHA generally transmits fewer packets than CRA ALOHA when the packet loss rate is low. On the contrary, as the packet loss rate increases, CRA ALOHA exhibits a more graceful degradation, leading to a lower average number of transmitted packets compared to BSS ALOHA.

TABLE I: Simulation parameters for different ALOHA schemes.

Quantity	BSS ALOHA	CRA ALOHA	CRA+BSS ALOHA
M	256	256	256
SNR	10 dB	10 dB	10 dB
N_P	0	64	64
N_D	$\{128, 256\}$	$\{128, 256\}$	$\{128, 256\}$
N_S	$\{195, 97\}$	$\{130, 78\}$	$\{130, 78\}$
R	$\{1, 2, 3\}$	$\{1, 2, 3\}$	$\{1, 2, 3\}$
N_T	4	Not Applicable	4

V. Conclusion

This paper explored the integration of BSS into a CRA ALOHA framework for massive machine-type communications. A novel scheme was proposed to effectively incorporate BSS, aiming to enhance conflict resolution among users. Through simulation analysis, the proposed approach demonstrated improved performance compared to conventional CRA ALOHA methods and ALOHA methods based solely on BSS. The results highlight the potential of BSS in enhancing the efficiency of diversity ALOHA, offering a promising direction for future research in large-scale random access systems.

References

[1] E. Paolini, C. Stefanovic, G. Liva, and P. Popovski, "Coded random access: Applying codes on graphs to design random access protocols," *IEEE Commun. Mag.*, vol. 53, no. 6, pp. 144–150, 2015.

[2] J. H. Sørensen, E. De Carvalho, Č. Stefanovic, and P. Popovski, "Coded pilot random access for massive MIMO systems," *IEEE Trans. Wireless Commun.*, vol. 17, no. 12, pp. 8035–8046, 2018.

[3] A. Munari, "Modern random access: An age of information perspective on irregular repetition slotted ALOHA," *IEEE Trans. Commun.*, vol. 69, no. 6, pp. 3572–3585, 2021.

[4] L. Valentini, M. Chiani, and E. Paolini, "Massive grant-free access with massive MIMO and spatially coupled replicas," *IEEE Trans. Commun.*, vol. 70, no. 11, pp. 7337–7350, 2022.

[5] L. Valentini, E. Bernardi, and E. Paolini, "Exploiting pilot mixtures in coded random access," *IEEE Communications Letters*, 2023.

[6] L. Valentini, M. Chiani, and E. Paolini, "Interference cancellation algorithms for grant-free multiple access with massive MIMO," *IEEE Trans. Commun.*, vol. 71, no. 8, pp. 4665–4677, 2023.

[7] A. K. Gupta and T. Venkatesh, "Design and performance evaluation of successive interference cancellation based Slotted Aloha MAC protocol," *Physical Communication*, vol. 55, p. 101910, 2022.

[8] J. Haghighat and T. M. Duman, "An energy-efficient feedback-aided irregular repetition slotted ALOHA scheme and its asymptotic performance analysis," *IEEE Trans. Wireless Commun.*, vol. 22, no. 12, pp. 9808–9820, 2023.

[9] D. Godard, "Self-recovering equalization and carrier tracking in two-dimensional data communication systems," *IEEE Trans. Commun.*, vol. 28, no. 11, pp. 1867–1875, 1980.

[10] J. Treichler and B. Agee, "A new approach to multipath correction of constant modulus signals," *IEEE Trans. Acoust., Speech, Signal Process.*, vol. 31, no. 2, pp. 459–472, 1983.

[11] M. Godeas, A. Carini, and F. Babich, "Blind source separation for ALOHA massive machine type communications," in *IEEE 101st Veh. Tech. Conf., VTC2025-Spring*, 2025.

[12] L. Valentini, A. Faedi, M. Chiani, and E. Paolini, "Coded random access for 6G: Intra-frame spatial coupling with ACKs," in *2021 IEEE Globecom Workshops (GC Wkshps)*. IEEE, 2021, pp. 1–6.

[13] T. Adali and P. J. Schreier, "Optimization and estimation of complex-valued signals: Theory and applications in filtering and blind source separation," *IEEE Signal Process. Mag.*, vol. 31, no. 5, 2014.

[14] V. Zarzoso and P. Comon, "Optimal step-size constant modulus algorithm," *IEEE Trans. Commun.*, vol. 56, no. 1, pp. 10–13, 2008.

[15] A. Chevreuil and P. Loubaton, "Blind signal separation for digital communication data," in *Academic Press Library in Signal Processing*. Elsevier, 2014, vol. 2, pp. 135–186.